

1 **A new approach to modeling the behavior**
2 **of frozen soils**

3
4 **Ali Nassr**

5 Department of Engineering, University of Exeter, North Park Road, Exeter, EX4 4QF
6 Email address: adnn201@exeter.ac.uk
7

8 **Mahzad Esmaeili-Falak**

9 Department of Civil Engineering, Faculty of Geotechnical Engineering,
10 University of Tabriz, 29 Bahman Blvd, Tabriz
11 Email address: mahzad.ef@tabrizu.ac.ir
12

13 **Hooshang Katebi**

14 Department of Civil Engineering, Faculty of Geotechnical Engineering,
15 University of Tabriz, 29 Bahman Blvd, Tabriz
16 Email address: katebi@tabrizu.ac.ir
17

18 **Akbar Javadi (Corresponding author)**

19 Department of Engineering, University of Exeter, North Park Road, Exeter, EX4 4QF
20 Email address: A.A. Javadi@exeter.ac.uk
21

22
23
24
25
26
Tel: +44 1392 723640

27 **A new approach to modeling the behavior of frozen soils**

28 **Ali Nassr, Mahzad Esmaeili-Falak, Hooshang Katebi, Akbar Javadi**

29 **Abstract**

30 In this paper a new approach is presented for modeling the behavior of frozen soils. A data-
31 mining technique, Evolutionary Polynomial Regression (EPR), is used for modeling the
32 thermo-mechanical behavior of frozen soils including the effects of confining pressure, strain
33 rate and temperature. EPR enables to create explicit and well-structured equations representing
34 the mechanical and thermal behavior of frozen soil using experimental data.

35 A comprehensive set of triaxial tests were carried out on samples of a frozen soil and the data
36 were used for training and verification of the EPR model. The developed EPR model was also
37 used to simulate the entire stress-strain curve of triaxial tests, the data for which were not used
38 during the training of the EPR model. The results of the EPR model predictions were compared
39 with the actual data and it was shown that the proposed methodology can extract and reproduce
40 the behavior of the frozen soil with a very high accuracy. It was also shown that the EPR model
41 is able to accurately generalize the predictions to unseen cases. A sensitivity analysis revealed
42 that the model developed from raw experimental data is able to extract and effectively represent
43 the underlying mechanics of the behavior of frozen soils. The proposed methodology presents
44 a unified approach to modeling of materials that can also help the user gain a deeper insight
45 into the behavior of the materials. The main advantages of the proposed technique in modeling
46 the complex behavior of frozen soil have been highlighted.

47

48 ***Key words:*** *frozen soils, soil modeling, triaxial test, data mining*

49

50 **1. Introduction**

51 Artificial ground freezing (AGF) has been extensively used in underground engineering. It has
52 negligible effects on the volume change of ground, adjacent buildings, groundwater,
53 surrounding soil and environment (Chamberlain 1981). Accurate determination of the shearing
54 behavior of frozen soils under different conditions and stress paths plays an important role in
55 the geotechnical construction projects such as open excavations, underground subway stations
56 and tunnels. Improper determination of the behavior of frozen soils could have disastrous
57 consequences as it could lead to underestimation of the allowable shear strength under loading
58 conditions of a particular application.

59 In AGF, artificial withdrawal of heat temporarily freezes the in-situ soil which leads to
60 stabilization of the soil mass such that the closed frozen bodies are watertight (Ziegler et al.
61 2013). One of the main benefits of AGF is that frozen bodies can be produced in all soil
62 conditions such as heterogeneous, soft and loose soils. AGF is an eco-friendly method, because
63 during implementation, there is no environmental impact on the soil and groundwater (Harris,
64 1995). It should be noted that AGF in geotechnical engineering should not be mistaken for
65 natural earth freezing or permafrost freeze-thaw cycles (Wang et al. 2016). AGF is the
66 deliberate freezing of pore water of soil which leads to increase in shear strength and reduction
67 in permeability.

68 In the last decade, AGF has been used as a method for temporary stabilization and hydraulic
69 sealing in different areas (Johansson, 2009). The mechanical behavior of unfrozen soils has
70 been extensively investigated by many researchers, however, there has been more limited
71 research on the behavior of frozen soils. Frozen soils exhibit higher strength under loading
72 compared with unfrozen soils (Czurda & Hohmann 1997). They also show similarity with ice
73 behavior in terms of a time dependent creep and their frictional properties like unfrozen phase
74 (Ma and Chang 2002). Frozen soil can be considered as a complex multiphase material

75 consisting of soil particles, frozen water, unfrozen water and air (Lackner et al., 2005). Some
76 researchers have studied the mechanical behavior of frozen soils through laboratory
77 experiments (Yang et al. 2010, Esmaeili-falak et al. 2017, Xu et al. 2017) . AGF was first
78 applied on a mine shaft project near Swansea, South Wales, in 1862 (Li et al., 2006).

79 Zhang et al. (2007) carried out extensive experimental work on frozen sand under different
80 confining pressures (CPs) using a triaxial apparatus. The results showed that volume of frozen
81 soils changed with temperature, confining pressure and soil type. It was also concluded that
82 during shearing, the average cross-sectional area increased nonlinearly with increasing axial
83 strain and confining pressure. Xu et al. (2011) investigated the behavior of ice saturated frozen
84 soil through a series of triaxial compression tests. The results showed that with increasing CP,
85 the shear strength changed during three distinct phases. They used improved Duncan-Chang
86 nonlinear model to analyze the stress–strain behavior. The results showed that the softening
87 behavior could be accurately described using this model.

88 In addition to the stress-strain behavior of frozen soils, the thermal gradient plays an important
89 role in stability analysis of geotechnical projects involving artificial ground freezing.

90 Zhao et al., (2013a) carried out a series of triaxial compression tests on a clay soil frozen with
91 non-uniform temperature, by using two methods under different CPs and thermal gradients: (i)
92 with K_0 consolidation (where the lateral strains were constrained) (K_0 DCGF), and (ii) without
93 K_0 consolidation (GFC). The results showed that the compressive strength of frozen clay
94 increases with increasing CP in the K_0 DCGF test, however, it decreases with increasing CP in
95 the GFC test. It was also shown that at a constant CP, the compressive strength of frozen clay
96 decreases with increasing thermal gradient in both K_0 DCGF and GFC tests. In the K_0 DCGF
97 test, the interaction between soil particles and pore ice significantly influences the strength of
98 the frozen clay.

99 Zhao et al. (2013b) conducted a further set of uniaxial compression tests applying different
100 average temperatures and thermal gradients on a frozen saturated clay. The results showed that
101 the uniaxial stress-strain curve of the frozen clay exhibit a linear elastic with strain hardening
102 behavior due to the effect of thermal gradient. It was also shown that decrease in average
103 temperature and thermal gradient increases the hardening behavior and uniaxial compressive
104 strength; but the elastic modulus varies slightly as the thermal gradient increases.

105 Yang et al. (2016) investigated the behavior of a frozen silt in a series of experimental tests
106 under various CPs and at temperatures between -2 to -8 °C. The output of this work showed
107 that the mechanical properties of frozen silt were highly influenced by CP and temperature.
108 The stress-strain curves presented strain softening behavior through the shearing stage
109 particularly at low CPs. However, by increasing CP, the strain softening decreased; and the
110 curves moved towards strain hardening at high CPs.

111 Over the last few years, several attempts have been made to develop constitutive and numerical
112 models for frozen soils. Yang et al. (2010) presented a constitutive model based on
113 experimental results using the Lade-Duncan strength function in π -plane and in p-q-plane
114 together. In this research, an elasto-plastic model was proposed to simulate the non-linear
115 behavior of frozen silt. This constitutive model employed yield surfaces with non-associated
116 flow rule for compressive and shear behavior. The actual and model predicted results were
117 compared showing a close agreement under low and high confinement.

118 Lai et al. (2016) presented a constitutive model for frozen saline soil based on a series of triaxial
119 compression tests. The developed model involved the effect of salt content on frozen soil
120 properties. They showed that the developed model can represent the mechanical behavior of
121 the soil with both straight and curved critical state lines as well as predicting the deformation
122 of such soils.

123 Rotta Loria et al., (2017) introduced a nonlinear elastic plastic model with associated flow rule,
124 which is able to simulate the non-linear behavior of frozen silt. The validity of the developed
125 model was verified using data obtained through triaxial tests from the literature, and it was
126 shown that it can reasonably predict the nonlinearity of the behavior of frozen silt at low and
127 high confinement.

128 Xu et al. (2017) proposed an elasto-plastic model to describe the behavior of frozen Helin
129 Loess, considering the effects of strain rate and temperature. The experimental results revealed
130 that the stress-strain curves of saturated frozen Helin loess exhibited strain-softening behavior
131 due to the temperature and strain rate conditions applied in the tests. The model parameters
132 were identified by fitting the experimental data. Comparing the experimental and simulated
133 results showed a close agreement and it was shown that the constitutive model can predict the
134 behavior of frozen Helin loess with reasonable accuracy.

135 Recently, with the developments in the computational field (software and hardware) some
136 researchers (e.g. Jahed Armaghani et al., 2015; Momeni et al., 2014) have emphasized on the
137 use of soft computing techniques such as the Simple Regression Analysis (SRA), Multiple
138 Regression Analysis (MRA) and Artificial Neural Network (ANN) in geotechnical engineering
139 problems. Data-driven models provide reasonable, quick and rigorous tools for solving wide
140 range of engineering problems, in particular when the relations between independent and
141 dependent parameters are unknown and complex. Furthermore, from the cost view point, these
142 methods are helpful as direct determination of behavior of frozen soils in laboratory is costly.
143 To the authors' knowledge, no previous research has been reported on the application of
144 artificial intelligence techniques to describe the constitutive behavior of frozen soils.

145 However, extensive research has been done on the use of artificial intelligence in modelling
146 the behavior of unfrozen soils and rocks (e.g. Millar, 2008; Monjezi and Rezaei, 2011).

147 In this paper, a data-mining technique is presented for modeling of the thermo-mechanical
148 behavior of frozen soil including the influences of strain rate, confining pressure, and
149 temperature on the soil behavior. The data mining model used is the evolutionary polynomial
150 regression (EPR), which is considered as a gray box model as it can generate relatively simple
151 mathematical structures to describe the behavior of a system (as opposed to black box models
152 like artificial neural network (ANN) that generates large complex structures (Rezania et al.,
153 2008). A comprehensive set of triaxial tests is conducted on soil samples taken from Line 2 of
154 Tabriz urban railway, Tabriz, East Azerbaijan province, Iran (from 38° 04' 34.9" N and 46° 12'
155 50.3" E to 38° 02' 30.91" N and 46° 24' 53.9" E) and the data are used to develop and validate
156 the proposed EPR model. This model is developed according to an incremental strategy using
157 six input parameters (temperature, confining pressure, strain rate, axial strain, axial strain
158 increment and devatoric stress) and one output parameter (devatoric stress for next increment).
159 The model is also used to produce the stress-strain curve of triaxial tests.

160

161 **2. Triaxial experiments**

162 Triaxial testing can be used to determine the mechanical behavior of frozen soils. In this
163 research triaxial compression tests have been conducted using standard procedures according
164 to ASTM D4083 (D4083-89, 2016). However, there are some challenges in direct
165 determination of behavior of frozen soils in the laboratory. For example, despite significant
166 developments in hardware, software and methods of laboratory testing of soils under various
167 conditions, preparing the triaxial apparatus for testing of frozen soils is often difficult, as it is
168 an expensive and unconventional geotechnical test.

169

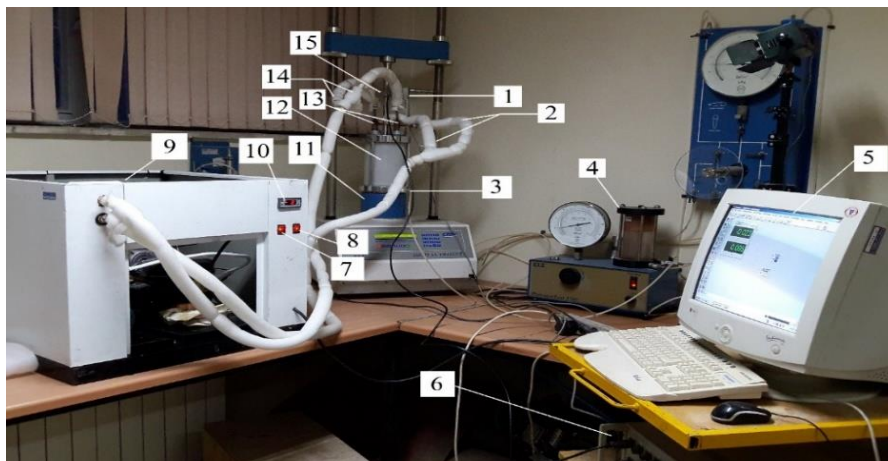
170

171 There are very few institutions with the facilities and capability to carry out experiments on
172 frozen soils (Pimentel and Anagnostou, 2010).

173 Another problem in laboratory simulation of AGF is that, it requires a cold and insulated room
174 with minimal heat transfer (Da Re et al. 2003). Also, the test procedure is very time consuming
175 and expensive (Ziegler et al., 2009). Considering these difficulties, in the present research a
176 triaxial compression test apparatus for frozen soils was designed and fabricated (Fig 1). A
177 comprehensive program of tests was carried out in an insulated cold room in the Department
178 of Civil Engineering at Tabriz University, where the temperature of the room was constantly
179 monitored and controlled.

180

181



182

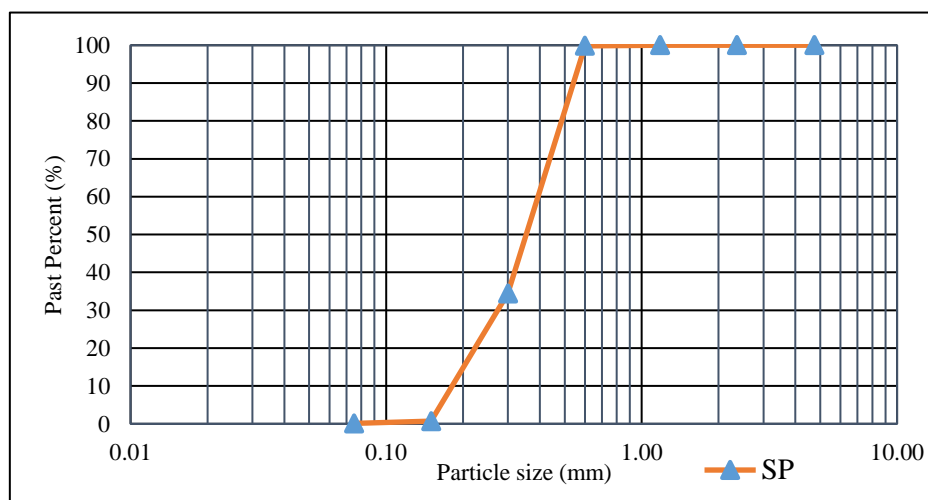
183 **Figure 1.** Triaxial compression test apparatus for frozen soils: (1) LVDT, (2) coolant output, (3)
184 confining pressure valve, (4) confining pressure system, (5) computer system, (6) data acquisition,
185 (7) pump power, (8) cooling power, (9) cooling machine, (10) thermostat-thermometer, (11) deviator
186 stress system, (12) triaxial chamber, (13) thermal transducer, (14) coolant input, (15) load cell.

184

185

186

187 Samples from the borehole core were transported to the geotechnical laboratory of the
188 University of Tabriz to determine the mechanical parameters of the frozen soil under different
189 conditions (confining pressure, strain rate and temperature). Based on some initial tests on the
190 unfrozen soil samples, the soil was classified as poorly graded sand (SP) according to the
191 United Soil Classification System (USCS) with ASTM D2487 (D2487, 2007). The gradation
192 curve of the soil is shown in Fig 2. From triaxial tests on the unfrozen soil samples, the cohesion
193 intercept and the angle of shearing resistance of the soil were determined as 0 and 33°,
194 respectively. The physical properties of the soil are presented in Table 1. As the soil is
195 cohesionless, due to the problems of obtaining identical and repeatable samples and the
196 inevitable disturbance during transportation and testing of the samples, it was decided to
197 prepare remolded soil samples according to the compaction and site conditions in order to
198 ensure reproducibility and comparability of the results.



199
200 **Figure 2.** Particle size distribution of frozen soil.
201
202
203

204 Table 1 Physical properties of SP soil.

Soil classification	SP
Saturated density (Mg/m ³)	1.98
Angle of friction (degree)	33
Specific gravity (Gs)	2.635
Gravel (%)	0
Sand (%)	98.8
Clay and silt (%)	1.2
Coefficient of uniformity (Cu)	2.17
Coefficient of curvature (Cc)	1.04

205

206 Remolded soil samples with the same void ratio and degree of saturation of ice were used, so
207 that a regular void ratio and saturation of 100% were considered. The prepared soils were cured
208 in split aluminum molds which were insulated from the bottom and top, so, freezing was
209 propagated in the radial direction in all of the samples (Fig. 3). The freezing process was so
210 rapid that no ice lenses were formed. Five percent of the samples were split before the testing
211 to monitor the absence of ice lenses.

212



213

214

Figure 3. Curing mold used for sample preparation.

215

216 After freezing, the specimens showed volumetric expansion in the longitudinal axis from the
217 top and bottom faces. The top and bottom surfaces of the samples were levelled with spiral
218 grinding machine. A total of 82 frozen sandy soil samples were prepared for the laboratory
219 tests. Unconsolidated undrained (UU) triaxial tests were chosen as an appropriate
220 representation of in situ conditions applied on the frozen samples under different conditions of
221 confining pressure, strain rate and temperature. The results showed a strain-softening behavior
222 for all specimens in all the tests.

223

224 **3. Evolutionary polynomial regression (EPR)**

225 EPR is a new hybrid data mining algorithm, based on an evolutionary computational procedure.
226 When applied to material modeling, its target is to find the best polynomial equation
227 representing the behavior of the material in a unified framework (Giustolisi and Savic, 2006).
228 The main advantages of the polynomial structures have been utilized in this algorithm to
229 develop a model in an appropriate mathematical form. The main feature of EPR is to use a
230 genetic algorithm (GA) to find out the more suitable exponents of the polynomial expressions.
231 This gives an efficient search for explicit equations which can represent the behavior of a
232 system and offers more control on the complexity of the structures generated. It also simplifies
233 the computational implementation of the algorithm (Giustolisi and Savic, 2006). The general
234 structure of EPR can be stated as

$$235 \quad Y = \sum_{j=1}^m F(\mathbf{X}, f(\mathbf{X}), a_j) + a_0 \quad (1)$$

236 where Y represents the output ; a_j is a constant parameter; F is a function built during the
237 analysis; X is the input variables matrix; f is a function that can be identified by the user (which
238 could include no function, logarithmic, exponential, tangent hyperbolic and secant hyperbolic),

239 and m is the number of terms of expression excluding the bias term (a_0) (Giustolisi and Savic,
 240 2006).

241 The EPR procedure starts with identifying a model form by transferring equation (1) to the
 242 following form:

$$243 \quad Y_{N \times 1}(\Theta, Z) = [I_{N \times 1} \quad Z^j_{N \times m}] \times [a_0 \quad a_1 \quad \dots \quad a_m]^T = Z_{N \times d} \times \Theta^T_{d \times 1} \quad (2)$$

244 where $Y_{N \times 1}(\Theta, Z)$ is the vector of N target values; $\Theta_{d \times 1}$ is the vector of $d = m + 1$ parameters a_j ,
 245 $j = 1:m$ and a_0 ; $Z_{N \times d}$ is a matrix form generated by 1 (unitary vector) for bias a_0 and m vectors
 246 of variables Z^j . for a fixed j , variables Z^j are a product of the independent predictor vectors of
 247 inputs, $X = \langle X_1 X_2 \dots X_k \rangle$ (Giustolisi and Savic, 2006).

248 Generally, EPR consists of two steps to build up a mathematical model. In the first step, a GA
 249 is used to search for the best equation form, which is a combination of vectors of independent
 250 input parameters, $X_s = 1:k$, and in the second step, the least square technique is used to find the
 251 adjustable parameters (Θ) for every single combination of inputs. A global search procedure is
 252 incorporated for the best set of input parameters and the corresponding exponents
 253 simultaneously based on a cost function specified by the user (Giustolisi and Savic, 2006). The
 254 matrix form of input variables (X) can be presented as:

$$255 \quad X = \begin{bmatrix} X_{11} & X_{12} & X_{1k} \\ X_{21} & X_{22} & X_{2k} \\ \dots & \dots & \dots \\ X_{N1} & X_{N2} & X_{NK} \end{bmatrix} = [X_1 \quad X_2 \quad X_3 \dots \dots X_k] \quad (3)$$

256 where the k^{th} column is the candidate variables for the j^{th} term in eq. (2), which can be written
 257 as:

258

259

260 $Z^j_{N \times l} = [(X_1)^{ES(j,1)} . (X_1)^{ES(j,2)} \dots \dots (X_k)^{ES(j,k)}]$ (4)

261 Z^j is the j^{th} column vector and their members are products of independent inputs variables, ES
 262 is a matrix of proposed exponents. The target of algorithm is to find the matrix $ES_{k \times m}$ of
 263 exponents in a range specified by the user.

264 The general framework of the EPR algorithm is shown in Figure 4. More details on the EPR
 265 method can be found in Doglioni et al. (2008) and Giustolisi and Savic, (2009, 2006). EPR can
 266 work with single or multi-objective optimization in order to represent the best symbolic
 267 equation (Giustolisi and Savic, 2009). In this work a multi-objective strategy is utilized to
 268 develop the EPR models. The accuracy of the EPR models is calculated based on the coefficient
 269 of determination (*CoD*) as:

270 $CoD = 1 - \frac{\sum_n (Y_a - Y_p)^2}{\sum_n (Y_a - \frac{1}{N} \sum_n Y_a)^2}$ (5)

271 where Y_a is the actual data; Y_p is the corresponding predicted data and N is the number of data
 272 points on which the *CoD* is evaluated (Giustolisi and Savic, 2009, 2006).

273

274

275

276

277

278

279

280

281

282

283

284

285

286

287

288

289

290

291

292

293

294

295

296

297

298

299

300

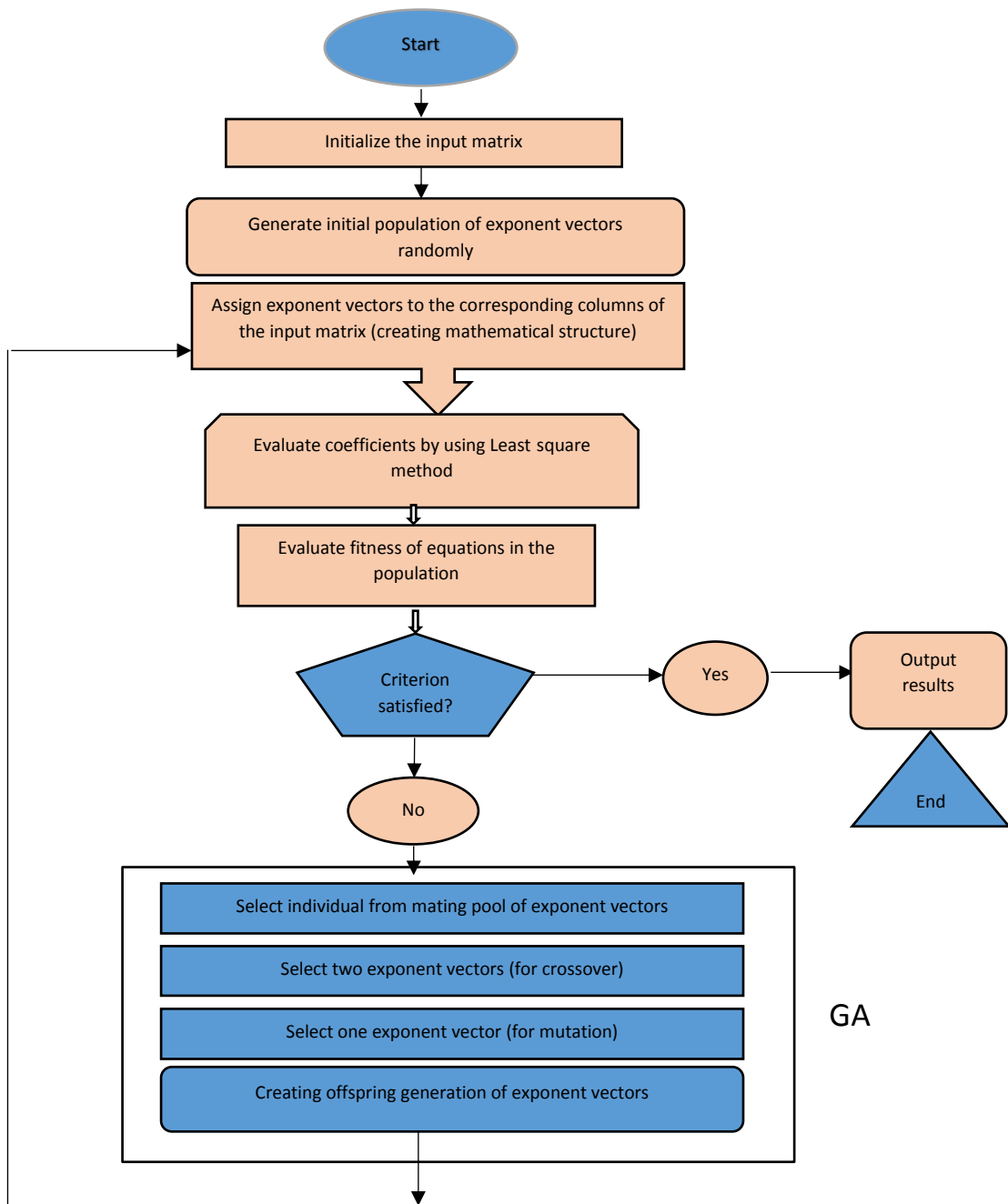


Figure 4. Flow diagram representing the EPR procedure (Doglioni et al., 2008).

301 **4. EPR based material modeling**

302 EPR has been successfully applied to a range of engineering applications. It is an effective tool
303 which is able to overcome some of the drawbacks in other types of data mining techniques such
304 as neural network and genetic programming (Javadi et al., 2012; Rezaia; et al., 2008). An EPR
305 based model has many advantages in representing the behavior of complex materials. It
306 provides a unified approach to material modelling and can be considered as the shortest path
307 from experiments to numerical modelling as it learns the material behavior from experimental
308 or field data directly without any assumptions (Rezaia; et al., 2008). Models developed by
309 EPR provide explicit mathematical equations that give the user a good understanding of the
310 effect of input variables on the predicted output. EPR was first used for environmental
311 modeling by Doglioni et al. (2008). Its application was then extended to various civil
312 engineering problems including geotechnical engineering (Ahangar-Asr et al., 2011; Alangar-
313 Asr; and Javadi, 2011; Rezaia; et al., 2008). EPR has been used to model the complex behavior
314 of saturated and unsaturated soils with very high accuracy. Results from a number of
315 comparative studies have shown that EPR models outperform ANNs (Ahangar-Asr et al., 2015;
316 Alani and Faramarzi, 2014; Javadi et al., 2012; Rezaia; et al., 2008).

317

318 **4.1 Training strategy**

319 Generally, there are two strategies (total stress-strain strategy and incremental stress-strain
320 strategy) that can be used to train EPR to generate a constitutive model representing the
321 material behavior (Faramarzi et al., 2012). In the first strategy, strains are used as input and
322 stresses as output. In the second strategy, the input and output data are used incrementally. In
323 this strategy the input data provide the EPR model with adequate information on the current
324 state of stresses and strains while the output parameter represents the next state of stress

325 corresponding to an input strain increment. The selection of an appropriate scheme for training
326 EPR models depends on several factors such as the source of data and the way the data are used
327 to train EPR. In this research the incremental strategy has been utilized for training of the EPR
328 models.

329 **4.2 Data preparation and EPR model**

330 Data from a comprehensive set of triaxial experiments on samples of frozen soil are used to
331 train an EPR-based model to predict the stress-strain behavior of the soil. The tests were
332 performed on samples of a sand compacted in the laboratory, under different confining
333 pressures, temperatures and strain rates. The testing program included unconsolidated
334 undrained triaxial (UU) tests where the axial strain was applied increasingly to shear the sample
335 under constant confining pressure. In the experiments, the samples were tested at temperatures
336 ranging between -0.5°C to -11°C and strain rates between 0.1 to 2 mm/min. The applied
337 confining pressures varied between 0 to 800 kPa. The dataset was divided into two groups, the
338 first group (80% of the data) was used for training of the EPR model, while the remaining (20%
339 of the) data, which was not used in the training stage, was used to validate the prediction
340 capability of the developed EPR model. In general, if a larger portion of data is used for
341 training, the accuracy of the training will improve. Many researchers have used about 80% of
342 the data for training and 20 % for testing (e.g. Ahangar-Asr et al., 2015; Alangar-Asr; and
343 Javadi, 2011; Rezania; et al., 2008). It was ensured that all parameters in the testing dataset lied
344 between the minimum and maximum values used in the training dataset to avoid extrapolation.
345 The incremental stress-strain strategy was employed in developing the EPR model. The EPR
346 model has six input variables as shown in Table (2). The input variables of the model are the
347 temperature, confining pressure, strain rate, current axial strain and current deviator stress, and
348 the models were developed to predict the deviator stress in the soil (model output) related to
349 an increment of axial strain.

350 The deviatoric stress and axial strain were updated incrementally through the training and
 351 testing stages based on output of the model at the end of each increment.

352 Table 2. The Input and output parameters used for developing the EPR model.

Type	Contributing parameters	Range
Input	Temperature (T)	-0.5 to -11 °C
	Confining pressure (σ_3)	0 to 800 kPa
	Strain rate ($\dot{\epsilon}$)	0.1 to 2 mm/min
	Axial strain (ϵ_y)	0 to 10%
	Axial strain increment ($\Delta\epsilon_y$)	0.1 to 0.4%
	Deviatoric stress (q)	0 to 12500 kPa
Output	Deviatoric stress for next increment (q_{i+1})	0 to 12500 kPa

353

354 In the EPR settings, the number of terms was set to 15 and the exponents were set to be in the
 355 range [0 1 2 3]. These settings were specified following a trial and error process of EPR runs.
 356 Before running the EPR all the datasets were randomly shuffled to ensure that the obtained
 357 EPR model was not biased towards a particular part of the training data. To reduce the required
 358 time for EPR training, duplicated data were removed. These steps were implemented through
 359 a code written in Matlab in order to simplify the training and reduce the time required for
 360 analysis. The best EPR model was selected according to the highest CoD (which was 99.88%)
 361 as:

$$\begin{aligned}
 362 \quad q_{i+1} = & 1.1053 q + 154078.5 \Delta\epsilon_y - 477650.84 T \Delta\epsilon_y^2 - 994036.26 \sigma_3 T \Delta\epsilon_y^3 \\
 363 \quad & - 27993.26 \epsilon_y - 1.449 \epsilon_y q + 12415.7 \dot{\epsilon} \epsilon_y + 242790.28 \epsilon_y^2 \quad (6) \\
 364 \quad & - 4446986.22 \Delta\epsilon_y \dot{\epsilon} \epsilon_y^2 - 2784857.5 \Delta\epsilon_y \dot{\epsilon} T \epsilon_y^2 + 57959.6 T \epsilon_y^3 \\
 365 \quad & - 0.0817 \sigma_3 \dot{\epsilon} q^2 \Delta\epsilon_y^3 - 34.09
 \end{aligned}$$

366 Figure 5 shows the deviator stress-axial strain curves predicted using the developed EPR model
 367 (equation 6) together with the actual experimental data used for the training process. It can be
 368 clearly seen that the proposed EPR model was able to extract the behavior of the frozen soil
 369 under different temperatures, strain rates and confining pressures with excellent accuracy.

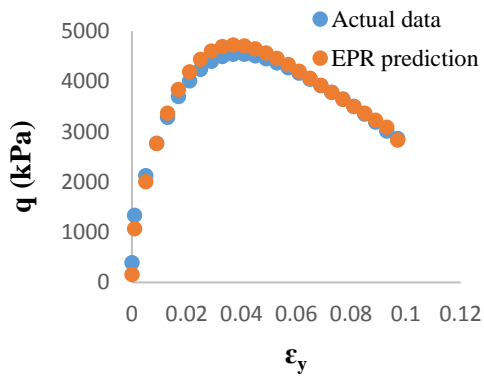
370

371

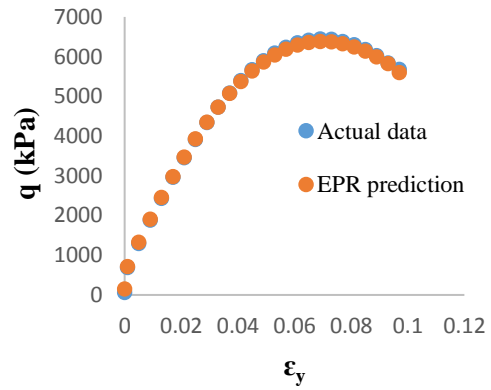
372

373

374



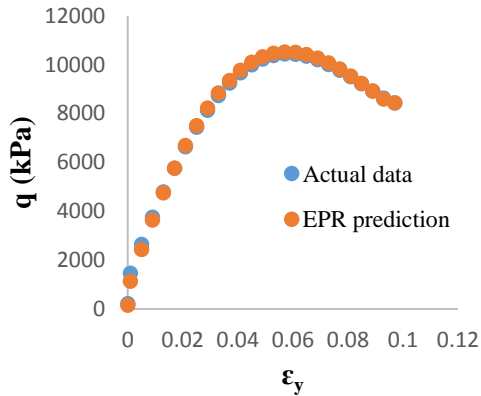
(a)



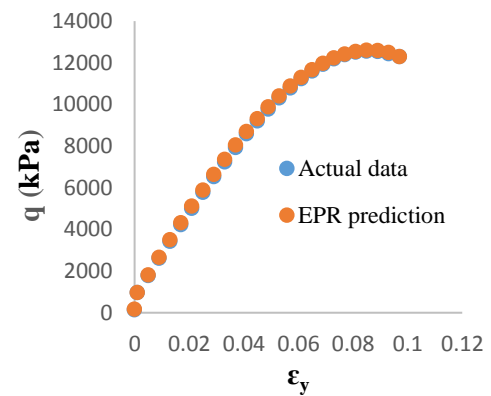
(b)

375

376



(c)



(d)

381

382

Figure 5. Comparison between the EPR model predictions and the experimental data for different confining pressures, temperatures and strain rates: (a) 100 kPa, -3 °C and 0.2 mm/min, (b) 50 kPa, -5 °C and 0.5 mm/min, (c) 800 kPa, -5 °C and 1.0 mm/min, (d) 200 kPa, -11 °C and 1.0 mm/min.

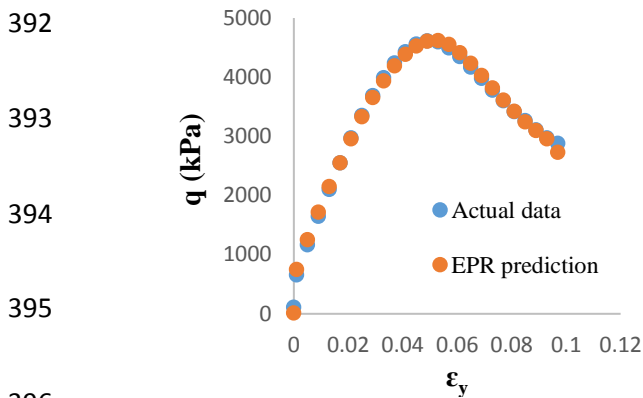
383

384

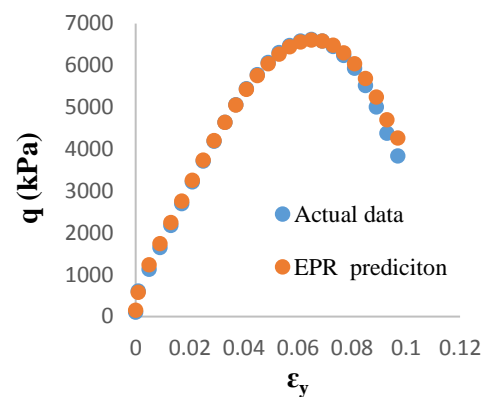
385

386 Moreover, to verify the generalization capability of the developed EPR model, the
 387 experimental results are compared with the EPR model predictions for the unseen (testing) data
 388 in Figure 6. The results show that the model is able to extend the learning and predict the
 389 behavior of the frozen soil under different temperatures, strain rates and confining pressures
 390 with very high accuracy.

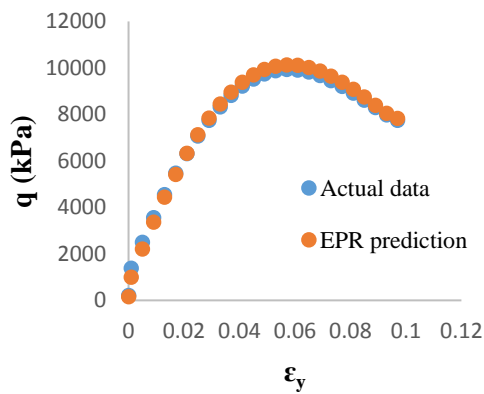
391



396



397



402

402

Figure 6 Comparison between the EPR model predictions and the (unseen) experimental data for different confining pressures, temperatures and strain rates: **(a)** 0 kPa, -5 °C and 0.2 mm/min, **(b)** 100 kPa, -2 °C and 1 mm/min, **(c)** 400 kPa, -5 °C and 1.0 mm/min.

404

405

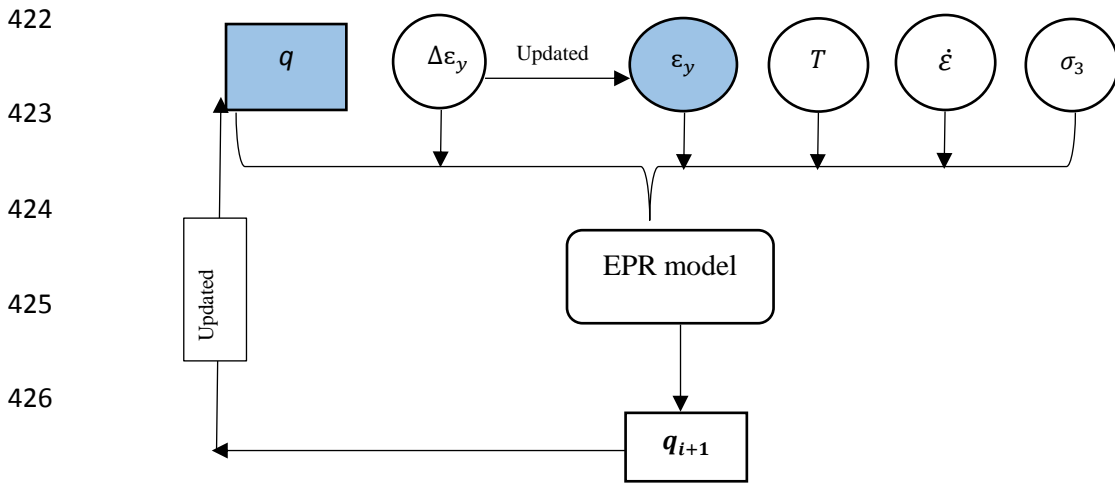
406

407 **5 Predicting the entire stress-strain curve using the EPR model**

408 Further to the model validation presented in section (4), the EPR model was utilized to predict
 409 the entire stress-strain curve in the $q: \epsilon_y$ space incrementally, point by point. The results from
 410 various sets of unseen (testing) data were used to measure the ability of the developed model
 411 to predict the behavior of the frozen soil, point by point, through the entire stress-strain curve.
 412 For each experiment, the magnitudes of temperature, strain rate and confining pressure were
 413 kept constant and the other parameters were updated incrementally based on the axial strain
 414 increment. Figure 7 shows the proposed procedure to update the input variables and build the
 415 whole stress-strain curve for the shearing stage of a triaxial experiment. Starting the procedure
 416 with zero axial strain and zero deviator stress (representing the starting point of the shearing
 417 stage) and using prescribed axial strain increment, the values of the deviator stress q_{i+1} are
 418 calculated using the developed EPR model (Ahangar-Asr et al., 2015; Faramarzi et al., 2012).
 419 For the next increment, the values of axial strain (ϵ_y) and deviator stress (q) are updated as:

420 $q_i = q_{i+1}$

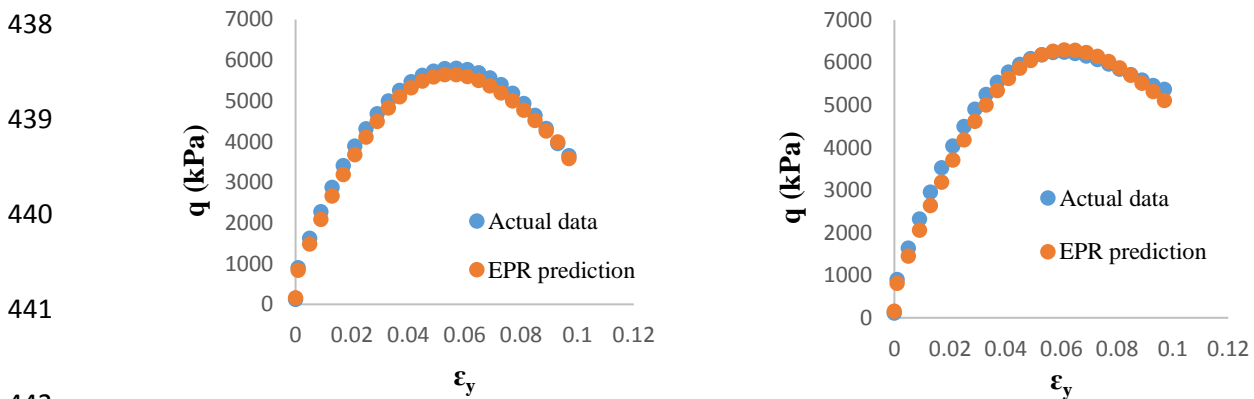
421 $\epsilon_{y,i} = \epsilon_{y,i} + \Delta\epsilon_y$



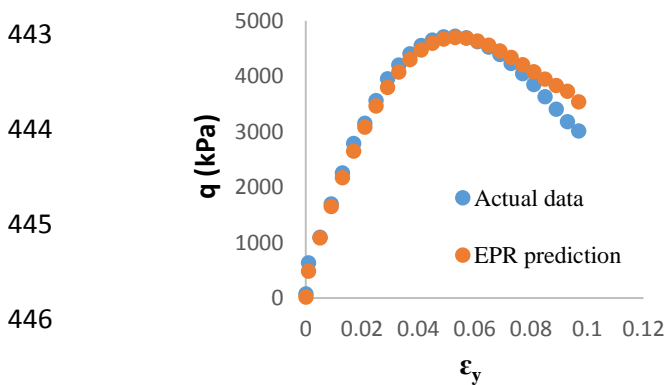
428 **Figure 7.** Procedure for predicting the entire stress-strain curve.

429 In this way, the next point on the axial strain – deviator stress curve is predicted. This algorithm
 430 was applied until all the points on the curve were predicted. Figure 8 shows the comparison
 431 between the three stress-strain curves predicted (point by point) by the EPR model and the
 432 experimental data. The results show very good agreement with the experimental results. The
 433 key point of such EPR model validation is that, while the errors were accumulated at every
 434 single point during the predictions, the entire curve was predicted very accurately. This is a
 435 strong testament of the robustness of the proposed EPR model in capturing and representing
 436 the real behavior of the frozen soil.

437



442



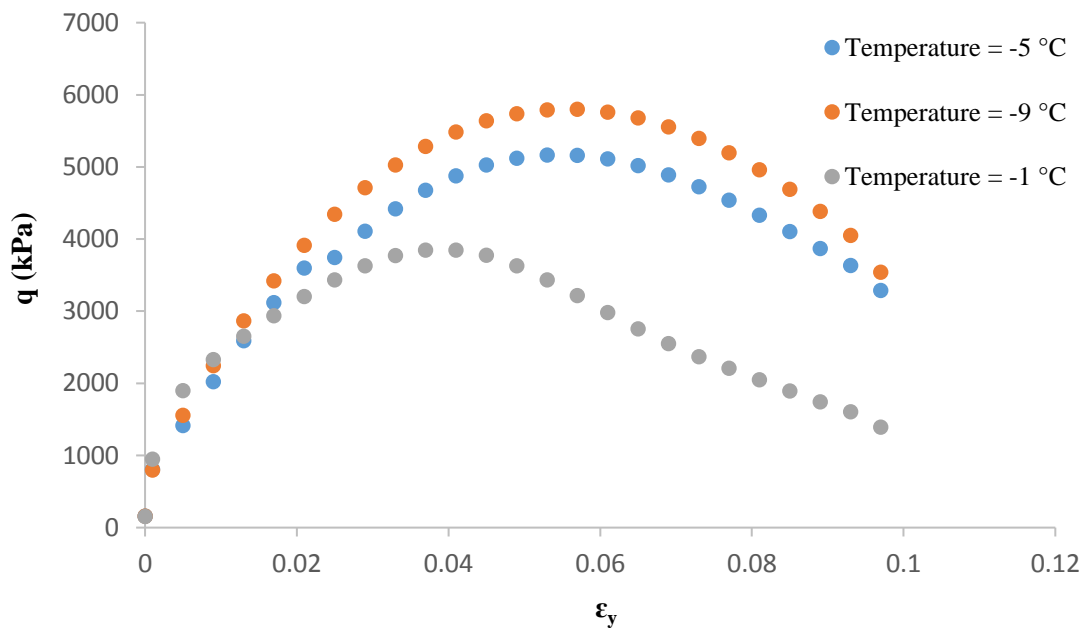
447

448 **Figure 8.** Comparison between the EPR model prediction (point by point) and the experimental
 449 data for confining pressures, temperatures and strain rates of (a) 0 kPa, -9 °C and 0.2 mm/min, (b)
 50 kPa, -4 °C and 0.5 mm/min, (c) 200 kPa, -3 °C and 0.2 mm/min.

450 **6 Sensitivity analysis**

451 A sensitivity analysis was conducted on the sets of validation (unseen) data. In this analysis,
452 changes were applied to the values of one selected input variable (within its maximum and
453 minimum range) while other input variables were fixed to their mean values. The analysis
454 included the effects of changes in confining pressure, temperature and strain rate on the
455 deviator stress - axial strain curve. Figures 9-11 show the effect of each input parameter on the
456 soil behavior. It can be seen that, as expected, decrease in temperature results in increase in the
457 deviator stress. Any increase in the confining pressure or strain rate would cause an increase in
458 the deviator stress. These results are expected and consistent with the trends noticed in the
459 experimental tests. The results of the sensitivity analysis indicate that the EPR model has been
460 able to extract and correctly predict the patterns of mechanical behavior of the frozen soil.

461



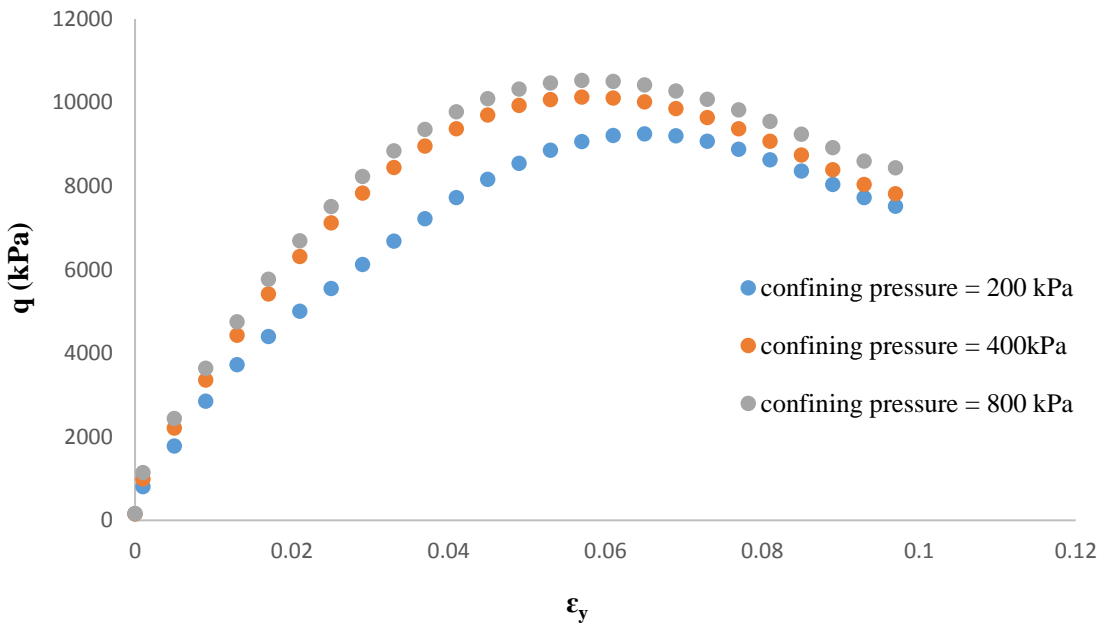
462

Figure 9. Effect of change in temperature on the behaviour of the frozen soil.

463

464

465

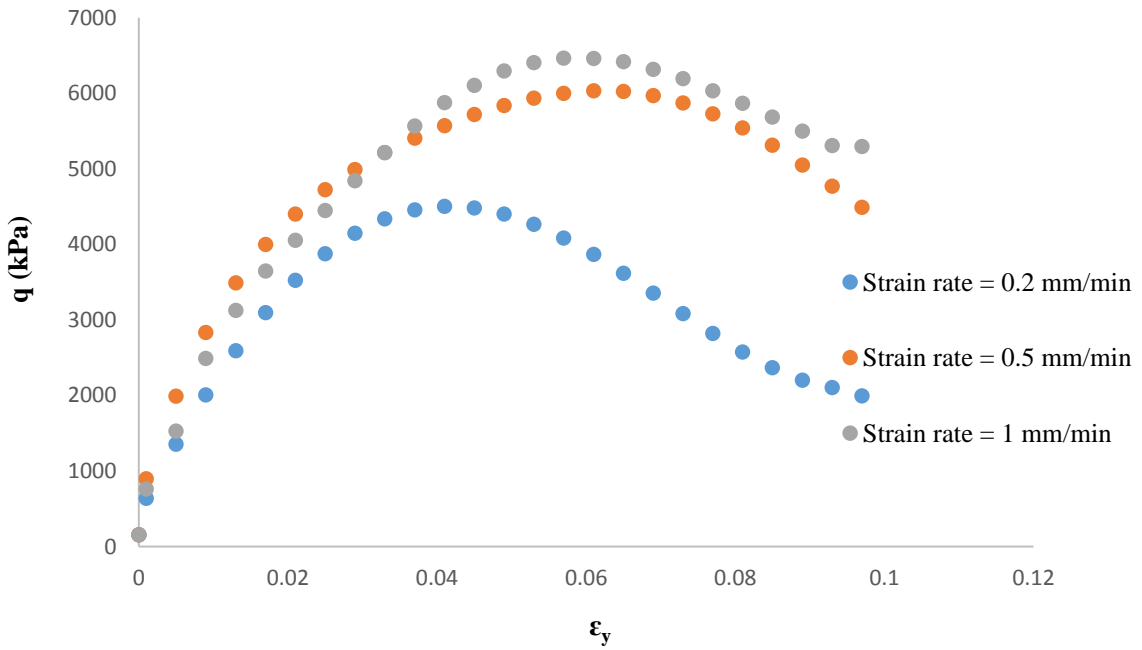


466

467

Figure 10. Effect of change in confining pressure on the behaviour of the frozen soil.

468



469

470

Figure 11. Effect of change in strain rate on the behaviour of the frozen soil.

471

472

473 **7. Discussion and conclusion**

474 The conventional approach to represent the mechanical behaviour of frozen soils requires
475 special equipment and environment which could be expensive, time consuming and not
476 available in all scenarios. In addition, the behaviour of such soils is very complex because of
477 the multi-phase nature of the mixture. In this paper, a comprehensive set of experimental data
478 from unconsolidated undrained (UU) triaxial tests on a frozen sandy soil were used to develop
479 a model, using evolutionary polynomial regression (EPR), to predict the shear behavior of a
480 frozen soil. The model considers the effects of temperature, confining pressure and strain rate
481 on the soil behavior. The main advantage of using EPR is that it provides a unified approach
482 to material modeling. It can also provide an explicit and well-structured model representing the
483 behavior of the material. EPR has several advantages over other types of data mining tools such
484 as neural network. It is able to extract simply the complex nonlinear behavior of different
485 materials by feeding it with large amount of data.

486 The methodology of using EPR-based model to describe the material behavior has been
487 verified by comparing the model predictions with the actual data and applying it on sets of
488 unseen data. The results showed the ability of the proposed model in capturing and representing
489 the complex behavior of frozen soils. Furthermore, predicting the entire stress-strain curve
490 (point by point) was presented successfully as another verification of the capabilities of the
491 developed model. A parametric analysis was introduced to assess the sensitivity of the
492 developed EPR model to variations of the individual variables including temperature, confining
493 pressure and strain rate. The results showed the EPR model is able to extract and predict the
494 effect of each parameter on the entire shear-stress curve of frozen soil. It should be noted that,
495 like other data mining techniques, a trained EPR model may be unable to accurately predict the
496 material behaviour outside the range of the training data.

497 In such cases, the predicted results should be treated with caution. In practice, the developed
498 model can be used to predict the response of frozen ground in projects involving ground
499 freezing. The model will provide a better insight into the behaviour of frozen soils in
500 engineering applications. The developed model can be implemented in numerical analysis such
501 as finite element method. The incorporation of the developed EPR model into finite element
502 analysis is the subject of current research.

503

504 **References**

- 505 Ahangar-Asr, A., Faramarzi, A., Javadi, A.A., 2011. Modelling Mechanical Behaviour of Rubber
506 Concrete Using Evolutionary Polynomial Regression. *Int. J. Comput. Eng.* 28(4), 492–507.
- 507 Ahangar-Asr, A., Javadi, A.A., Khalili, N., 2015. An evolutionary approach to modelling the
508 thermomechanical behaviour of unsaturated soils. *Int. J. Numer. Anal. Methods Geomech.* 39,
509 539–557.
- 510 Alangar-Asr, Javadi, A.A., 2011. Modeling soil-water characteristic curve using EPR Modeling
511 characteristic curve using EPR. *Unsaturated Soils Theory Pract.* 2011 379–383.
- 512 Alani, A.M., Faramarzi, A., 2014. An evolutionary approach to modelling concrete degradation due to
513 sulphuric acid attack. *Appl. Soft Comput. J.* 24, 985–993. doi:10.1016/j.asoc.2014.08.044
- 514 Chamberlain, E.J., 1981. Overconsolidation effects of ground freezing. *Eng. Geol.* 18, 97–110.
- 515 Czurda, K. A., & Hohmann, M., 1997. Freezing effect on shear strength of clayey soils. *Appl. Clay*
516 *Sci.* 12(1), 165–187.
- 517 D2487, A.S., 2007. Standard practice for classification of soils for engineering purposes (unified soil
518 classification system). ASTM Int. West Conshohocken, PA.
- 519 D4083-89, A., 2016. Standard Practice for Description of Frozen Soils (Visual-Manual Procedure).
520 ASTM Int. West Conshohocken, PA.
- 521 Da Re, G., Germaine, J. T., & Ladd, C.C., 2003. Triaxial testing of frozen sand: Equipment and
522 example results. *J. cold Reg. Eng.* 17(3), 90–118.

- 523 Doglioni, A., Giustolisi, O., Savic, D.A., Webb, B.W., 2008. An investigation on stream temperature
524 analysis based on evolutionary computing. *Hydrol. Process.* 22(3), 315–326.
- 525 Esmaeili-falak, M., Katebi, H., Javadi, A., 2017. Experimental Study of the Mechanical Behavior of
526 Frozen Soils - A Case Study of Tabriz Subway. *Period. Polytech. Civ. Eng.* 1–9.
- 527 Faramarzi, A., Javadi, A.A., Alani, A.M., 2012. EPR-based material modelling of soils considering
528 volume changes. *Comput. Geosci.* 48, 73–85. doi:10.1016/j.cageo.2012.05.015
- 529 Giustolisi, O., Savic, D.A., 2009. Advances in data-driven analyses and modelling using EPR-
530 MOGA. *J. Hydroinformatics* 11, 225–236. doi:10.2166/hydro.2009.017
- 531 Giustolisi, O., Savic, D.A., 2006. A symbolic data-driven technique based on evolutionary polynomial
532 regression. *J. Hydroinformatics* 8, 207–222. doi:10.2166/hydro.2006.020
- 533 Harris, J.S., 1995. *Ground Freezing in Practice*. Thomas Telford, London., Harris, J. S. 1995. *Ground*
534 *Freezing in Practice*. Thomas Telford, London.
- 535 Jahed Armaghani, D., Tonnizam Mohamad, E., Momeni, E., Narayanasamy, M.S., Mohd Amin, M.F.,
536 2015. An adaptive neuro-fuzzy inference system for predicting unconfined compressive strength
537 and Young’s modulus: a study on Main Range granite. *Bull. Eng. Geol. Environ.* 74, 1301–
538 1319. doi:10.1007/s10064-014-0687-4
- 539 Javadi, A.A., Ahangar-Asr, A., Johari, A., Faramarzi, A., Toll, D., 2012. Modelling stress-strain and
540 volume change behaviour of unsaturated soils using an evolutionary based data mining
541 technique, an incremental approach. *Eng. Appl. Artif. Intell.* 25, 926–933.
542 doi:10.1016/j.engappai.2012.03.006
- 543 Johansson, T., 2009. *Artificial Ground Freezing in Clayey Soils: Laboratory and Field Studies of*
544 *Deformations during Thawing at the Bothnia Line*. Royal Institute of Technology, Stockholm,
545 Sweden.
- 546 Lackner, R., Amon, A., Lagger, H., 2005. Artificial Ground Freezing of Fully Saturated Soil: Thermal
547 Problem. *J. Eng. Mech.* 131(2), 211–220.
- 548 Lai, Y., Liao, M., Hu, K., 2016. A constitutive model of frozen saline sandy soil based on energy
549 dissipation theory. *Int. J. Plast.* 78, 84–113. doi:10.1016/j.ijplas.2015.10.008
- 550 Li, S., Lai, Y., Zhang, M., Zhang, S., 2006. Minimum ground pre-freezing time before excavation of
551 Guangzhou subway tunnel. *Cold Reg. Sci. Technol.* 46, 181–191.
552 doi:10.1016/j.coldregions.2006.09.001

- 553 Ma, W., Chang, X., 2002. Analyses of strength and deformation of an artificially frozen soil wall in
554 underground engineering. *Cold Reg. Sci. Technol.* 34(1), 11–17.
- 555 Millar, D.L., 2008. *Parallel Distributed Processing In Rock Engineering Systems*. PhD thesis,
556 Imperial College of Science, Technology & Medicine, London.
- 557 Momeni, E., Nazir, R., Armaghani, D.J., Maizir, H., 2014. Prediction of pile bearing capacity using a
558 hybrid genetic algorithm-based ANN. *Measurement* 57, 122–131.
559 doi:10.1016/j.measurement.2014.08.007
- 560 Monjezi, M., Rezaei, M., 2011. Developing a new fuzzy model to predict burden from rock
561 geomechanical properties. *Expert Syst. Appl.* 38, 9266–9273. doi:10.1016/j.eswa.2011.01.029
- 562 Pimentel, E., Anagnostou, G., 2010. Large-scale physical model for simulation of artificial ground
563 freezing with seepage flow. *7th Int. Conf. Phys. Model. Geotech.* 28th June - 1st July, Zurich,
564 Switzerland, CRC Press. Zurich,2010 379–382.
- 565 Rezania;, M., Javadi;, A., Orazio Giustolisi, 2008. An Evolutionary-Based Data Mining Technique for
566 Assessment of Civil Engineering Systems. *Eng. Comput. Int. J. Comput. aided Eng. Softw.* 25,
567 500–517.
- 568 Rotta Loria, A.F., Frigo, B., Chiaia, B., 2017. A non-linear constitutive model for describing the
569 mechanical behaviour of frozen ground and permafrost. *Cold Reg. Sci. Technol.* 133, 63–69.
570 doi:10.1016/j.coldregions.2016.10.010
- 571 Wang, S., Qi, J., Yu, F., & Liu, F., 2016. A novel modeling of settlement of foundations in permafrost
572 regions. *Geomech. Eng.* 10(2), 225–245.
- 573 Xu, X., Lai, Y., Dong, Y., Qi, J., 2011. Laboratory investigation on strength and deformation
574 characteristics of ice-saturated frozen sandy soil. *Cold Reg. Sci. Technol.* 69, 98–104.
575 doi:10.1016/j.coldregions.2011.07.005
- 576 Xu, X., Wang, Y., Yin, Z., Zhang, H., 2017. Effect of temperature and strain rate on mechanical
577 characteristics and constitutive model of frozen Helin loess. *Cold Reg. Sci. Technol.* 136, 44–51.
578 doi:10.1016/j.coldregions.2017.01.010
- 579 Yang, Y., Feng, G., Yuanming, L., Hongmei, C., 2016. Experimental and theoretical investigations on
580 the mechanical behaviors of frozen silt. *Cold Reg. Sci. Technol.* 130, 59–65.
581 doi:10.1016/j.coldregions.2016.07.008

582

- 583 Yang, Y., Lai, Y., Dong, Y., Li, S., 2010. The strength criterion and elastoplastic constitutive model
584 of frozen soil under high confining pressures. *Cold Reg. Sci. Technol.* 60, 154–160.
585 doi:10.1016/j.coldregions.2009.09.001
- 586 Zhang, S., Lai, Y., Sun, Z., Gao, Z., 2007. Volumetric strain and strength behavior of frozen soils
587 under confinement. *Cold Reg. Sci. Technol.* 47, 263–270.
588 doi:10.1016/j.coldregions.2006.10.001
- 589 Zhao, X., Zhou, G., Chen, G., 2013a. Triaxial compression strength for artificial frozen clay with
590 thermal gradient. *J. Cent. south Univ.* 20, 218–225. doi:10.1007/s11771-013-1479-x
- 591 Zhao, X., Zhou, G., Wang, J., 2013b. Deformation and strength behaviors of frozen clay with thermal
592 gradient under uniaxial compression. *Tunn. Undergr. Sp. Technol. Inc. Trenchless Technol. Res.*
593 38, 550–558. doi:10.1016/j.tust.2013.09.003
- 594 Ziegler, M., Schüller, R., & Mottaghy, D., 2013. Numerical simulation of energy consumption of
595 artificial ground freezing applications subject to water seepage, in: *In Proceedings of the 18th*
596 *International Conference on Soil Mechanics and Geotechnical Engineering: The Academia and*
597 *Practice of Geotechnical Engineering, Paris, France.* pp. 2985–2988.
- 598 Ziegler, M., Baier, C., Aulbach, B., 2009. Simplified phase change model for artificially frozen
599 ground subject to water seepage. *Proc. 17th Int. Conf. Soil Mech. Geotech. Eng. Acad. Pract.*
600 *Geotech. Eng. Alexandria, Egypt, 5-9 Oct. 2009.* 562–565. doi:10.3233/978-1-60750-031-5-562
- 601